Supplementary Information (SI) for Catalysis Science & Technology.

Supporting Information

IrRu nanoparticles boosted by Ir/Ru-N-C toward acidic hydrogen oxidation with high CO tolerance

Mengyu Yang,[a] Rui Gao,*[a] Shuo Han,[a] Zhongyu Qiu,[a] Chunxiao Chai,[a] Hao Yang,[a] Yang Zhao,[b] Ruijie Song,[a] Xihong Shen,[a] Xingchen Zeng,[a] Yujiang Song*[a]

[a] State Key Laboratory of Fine Chemicals, School of Chemical Engineering, Dalian University of Technology, 2 Linggong Road, Dalian, Liaoning, 116024, China.

[b] Dalian National Laboratory for Clean Energy, Dalian Institute of Chemical Physics, Chinese Academy of Sciences, Dalian, Liaoning, 116023, China.

E-mail: gaorui16@dlut.edu.cn; yjsong@dlut.edu.cn.

Chemicals

2-methylimidazole (2-MI, 99%) was obtained from J&K Scientific Ltd (China). Zinc acetate (≥99.0%) and polyvinylpyrrolidone (PVP, average mol. wt. 40,000) were purchased from Sigma-Aldrich (United States). Iridium(III) acetylacetonate (Ir(acac)$_3$, 98%) was obtained from Alfa Aesa (United Kingdom). Ruthenium(III) acetylacetonate (Ru(acac)$_3$, 98%) was received from Energy Chemical (China). Methanol (AR) and sulfuric acid (98%) were purchased from Tianjin Kemiou Chemical Reagent Co. Ltd (China). Ethanol (≥99.8%) was obtained from Sinopharm Chemical Reagent Co. Ltd (China). Commercial Pt/C (20 wt%), commercial Pt/C (60 wt%) and commercial PtRu/C (30 wt%) were received from Johnson Matthey Chemical Co. Ltd (United Kingdom). Gore membrane (M788.12) was purchased from W. L. Gore & Associates (United States). Nafion resin solution (D520, 5 wt% in mixture of lower aliphatic alcohols and water, contains 45% water) was ordered from DuPont (United States). Gas diffusion layer (GDL, 0.4875±0.03 mm in thickness) with microporous layer was obtained from Sunrise Power Co. Ltd (China). All the above chemicals were used as received without further purification. Carbon black (Ketjenblack EC600 JD) was obtained from Akzo Nobel (Netherlands) and pretreated with 3 M nitric acid aqueous solution (aq.) at 80 °C for 1 h before use. The ultrapure water (18.2 MΩ cm at 25 °C) was obtained from a Millipore water system (Synergy® UV, France) and used in all experiments.

Synthesis of IrRu@ZIF-8

In a typical synthesis, Ir(acac)$_3$ (19.58 mg, 0.04 mmol) and Ru(acac)$_3$ (7.97 mg, 0.02 mmol) were dissolved in 2 mL methanol and transferred to 2 mL 2-MI (1.3138 g, 16 mmol) aqueous solution. Next, 2 mL of Zn acetate (0.2195 mg, 1 mmol) and PVP (320 mg) aqueous solution was added in and vigorously stirred for 4 hours under ambient conditions. The orange-reddish precipitates were collected by centrifugation and washed four times with ultrapure water and dried overnight at 75 °C in an oven, denoted as IrRu@ZIF-8. The quantity of IrRu@ZIF-8 is about 30 mg. For comparison, Ir(acac)$_3$ and Ru(acac)$_3$ at different molar ratios (1:3, 1:2, 1:1, 3:1, and 1:0, as well as 0:1) were also used for the synthesis while holding the other synthetic parameters the same.

Synthesis of nanocomposite

The IrRu@ZIF-8 powder was placed in a tube furnace and heated to 900 °C for 2 h with a ramping rate of 5 °C min^{-1} from room temperature under argon atmosphere with a flow rate of 400 mL min^{-1}. After cooling down to room temperature naturally, the obtained powder was manually ground thoroughly for 2 min through an agate mortar with a dimeter of 60 mm. The quantity of the nanocomposite is about 5 mg with a pyrolysis yield of approximately 17%. For comparison, the pyrolysis temperature was changed in the range of 800 to 1000 °C.

Synthesis of IrRu/C

EC600 (26.4 mg) was dispersed in ultrapure water (25.4 mL) under mild sonication for 10 min, followed by the addition of $RuCl_3$ aq. (0.473 mL, 20 mM) and $IrCl_3$ aq. (0.662 mL, 20 mM) under mild sonication for 10 min. Next, the mixture was placed in an ice-water bath, and then freshly prepared ice-cold $NaBH_4$ aq. (1.135 mL, 150 mM) was added in and vigorously stirred for 1 h. Finally, the temperature of the reaction system was increased to 60 °C, and then freshly prepared $NaBH_4$ aq. (1.135 mL, 150 mM) was added to ensure the complete reduction of metal complexes. After 30 min of reaction at 60 °C, the product was collected by filtration and washed with ultrapure water until the filtrate became pH neutral. Then, the obtained black powder was dried overnight in an oven at 65 ◦C and manually ground thoroughly for 2 min through an agate mortar with a dimeter of 60 mm. The quantity of the product is about 24 mg. The as-prepared sample was heat-treated in argon atmosphere containing 5% H_2 at 120 °C for 2 h with a ramping rate of 5 °C min^{-1} and a flow rate of 400 mL min^{-1}. The pyrolysis yield is approximately 84%.

Characterizations

High resolution scanning transmission electron microscopy (HR-STEM), high-angle annular dark field-STEM (HAADF-STEM), energy dispersive X-ray spectroscopy (EDS) elemental mapping as well as linear scan profiles were recorded on a JEM-ARM200F (JEOL). The crystalline structures of the nanocomposite was analyzed by powder X-ray diffraction (XRD) on a Smart Lab 9 kW (Rigaku) operating at 45 kV and 200 mA with a scanning rate of 10° min^{-1}. Inductively coupled plasma-optical emission spectroscopy (ICP-OES) was carried out on an AVIO 500 (PerkinElmer). X-ray photoelectron spectroscopy (XPS) measurements were performed to determine the chemical bonding states using an ESCALAB XI+ (Thermo Scientific). A neutralizer was used for the XPS measurements and surface sp^2 C (C-H bond) was used to carry out the calibration.[1] *In-situ* attenuated total reflection surface-enhanced infrared absorption spectroscopy (ATR-SEIRAS) spectra were recorded on Fourier transform infrared (FTIR) spectrometer equipped with a mercury cadmium telluride (MCT) detector (Bruker).

Electrochemical measurements

All electrochemical measurements were performed on CHI760E electrochemical station (Shanghai Chenhua Instruments Ltd.) with a glassy carbon rotating disk electrode (RDE, 5 mm in diameter) as the working electrode (WE), a carbon rod as the counter electrode (CE), and a Hg/Hg_2SO_4 (saturated K_2SO_4) as the reference electrode (RE). The surface of RDE is polished with 30-50 nm alumina paste and then cleaned with ethanol and ultrapure water. The nanocomposite (5 mg) was dispersed in a mixed solvent of 950 μL ethanol and 50 μL Nafion resin solution (5 wt%), then sonicated for 20 min to form a homogeneous ink (5 mg mL^{-1}).[2] 20 μL of the ink was dropwise dropped on the surface of RDE. For comparison, 3 mg of commercial Pt/C (20 wt%) or commercial PtRu/C (30 wt%) was dispersed in the mixture of ultrapure water (300 μL), ethanol (2700 μL), and Nafion resin solution (5 wt%, 18 μL), then sonicated for 20 min to form a homogeneous ink (1 mg mL^{-1}).[3] 10 μL of the ink was dropped on the surface of RDE.

Cyclic voltammetry (CV) between 0-1.2 V vs. RHE with a scanning rate of 50 mV s^{-1} in N_2-saturated 0.5 M H_2SO_4 aq. was performed to clean the electrocatalysts surface. The HOR performance of the electrocatalysts was evaluated by linear sweep voltammetry (LSV) in H_2-saturated 0.5 M H_2SO_4 aq. at 25 °C from 0 to 0.5 V vs. RHE with a positive sweep rate of 10 mV s^{-1} and a rotation rate of 1600 rpm.

CO tolerance of the electrocatalysts was assessed by holding the WE at 0.1 V vs. RHE for 600 s in 1000 ppm CO/H_2-saturated 0.5 M H_2SO_4 aq. with subsequent LSV test from 0 to 0.5 V vs. RHE at a positive sweep rate of 10 mV s^{-1} and a rotation rate of 1600 rpm. Additionally, the CO tolerance was also evaluated by holding the WE at 0.1 V vs. RHE and a rotation rate of 1600 rpm with a chronoamperometry method for 2000 s in 1000 ppm CO/H_2-saturated 0.5 M H_2SO_4 aq.

The electrochemical active surface area (ECSA) was assessed by CO stripping in 0.5 M H_2SO_4 aq. at 25 °C. Firstly, CO was bubbled in 0.5 M H_2SO_4 aq. for 10 min to reach a full monolayer of adsorbed CO on the metal surface at 0.1 V vs. RHE. In the following, N_2 was bubbled for another 10 min to remove non-adsorbed CO. Finally, CO stripping was recorded by collecting CV between 0.05-1.2 V vs. RHE with a scanning rate of 20 mV s^{-1}. ECSA is calculated according to equation (S1):

$$\mathrm{ECSA} = \frac{\mathrm{Q_{CO}}}{\mathrm{C} \times \mathrm{m}} \tag{S1}$$

where, Q_{CO} is the integral charge of CO oxidation on the surface of electrocatalysts; C is the coulombic charge required for the oxidation of a monolayer of CO, where the C of Pt group metal is 420 μC cm^{-2}; m is the mass of metal on RDE.[4-7]

CO oxidation reaction (COOR) performance was measured by LSV in CO-saturated 0.5 M H_2SO_4 aq. at 25 °C from 0 V vs. RHE to 0.5 V vs. RHE with a positive sweep rate of 10 mV s^{-1} and a rotation rate of 1600 rpm.

For *in-situ* ATR-SEIRAS measurements, 30 μL of the nanocomposite ink was dropwise dropped on the Au-coated film on a silicon semi-cylindrical prism as the working electrode. A saturated calomel electrode (SCE, Hg/Hg_2Cl_2 with saturated KCl) and a carbon rod were used as reference and counter electrode, respectively. *In-situ* ATR-SEIRAS were recorded in CO-saturated 0.5 M H_2SO_4 aq. at 0, 0.1, 0.2, 0.3, and 0.4 V vs. RHE, respectively.

Membrane electrode assembly (MEA) fabrication and PEMFCs tests

The anodic nanocomposite ink was prepared by ultrasonicating the mixture of the nanocomposite (2 mg), Nafion resin solution (5 wt%, 22.7 μL), ultrapure water (100 μL), and ethanol (900 μL) for 20 min. Similarly, commercial 60 wt% Pt/C (2 mg) was dispersed in the mixture of ultrapure water (100 μL), ethanol (900 μL), and Nafion resin solution (5 wt%, 12.2 μL) under sonication for 20 min to prepare anodic Pt/C ink. The cathodic Pt/C ink was prepared by mixing commercial 60 wt% Pt/C (2 mg), ultrapure water (100 μL), ethanol (900 μL), and Nafion resin solution (5 wt%, 6.9 μL) under sonication for 30 min.

A spray gun with a 0.3 mm nozzle was used to manually spray the electrocatalyst ink. Firstly, the nanocomposite ink was sprayed onto the microporous layer side of GDL to attain a metal loading of 0.02 mg_{IrRu} cm^{-2}. Then, the anodic and cathodic Pt/C ink was sprayed onto each side of membrane with an active area of 1 cm^2 to attain an anodic and cathodic Pt loading of 0.1 mg_{Pt} cm^{-2} and 0.2 mg_{Pt} cm^{-2}, respectively. The membrane electrode was sandwiched in between the nanocomposite coated GDL and the other GDL under a pressure of 0.15 MPa for 3 min at 130 °C to form MEA as shown in Fig. S16. For comparison, Pt/C was fabricated into MEA using the same procedure as the above except by using pristine GDL instead of the nanocomposite coated GDL as shown in Fig. S17.

For further comparison, the nanocomposite (0.02 mg_{IrRu} cm^{-2})+commercial 30 wt% PtRu/C (0.1 mg_{PtRu} cm^{-2}), commercial 30 wt% PtRu/C (0.1 mg_{PtRu} cm^{-2}) by itself, and nanocomposite (0.1 mg_{IrRu} cm^{-2}) by itself were also fabricated as MEAs by using the same fabrication parameters as above.

The PEMFC single cells were tested at 80 °C and 100 % relative humidity (RH) with a back pressure of 150 kPa. The anode and the cathode was supplied with 50 ppm CO/H_2 at 100 mL min^{-1} and O_2 at 200 mL min^{-1}, respectively.

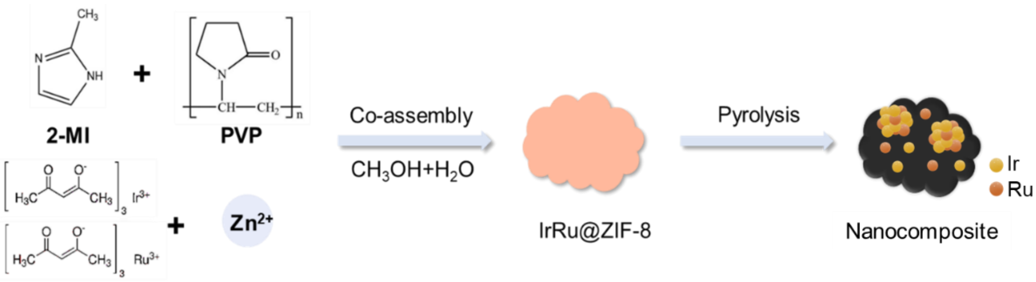

Figure S1 Schematic diagram of the synthetic process of the nanocomposite.

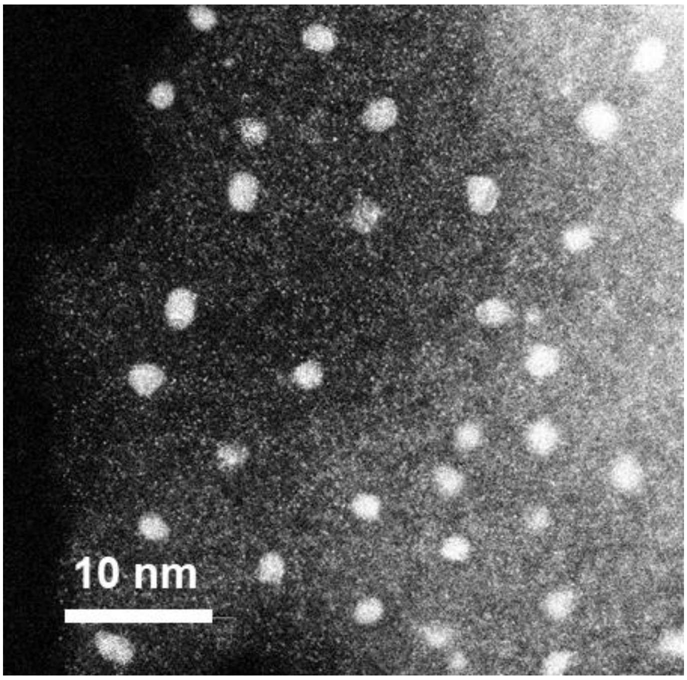

Figure S2 HAADF-STEM image of the nanocomposite.

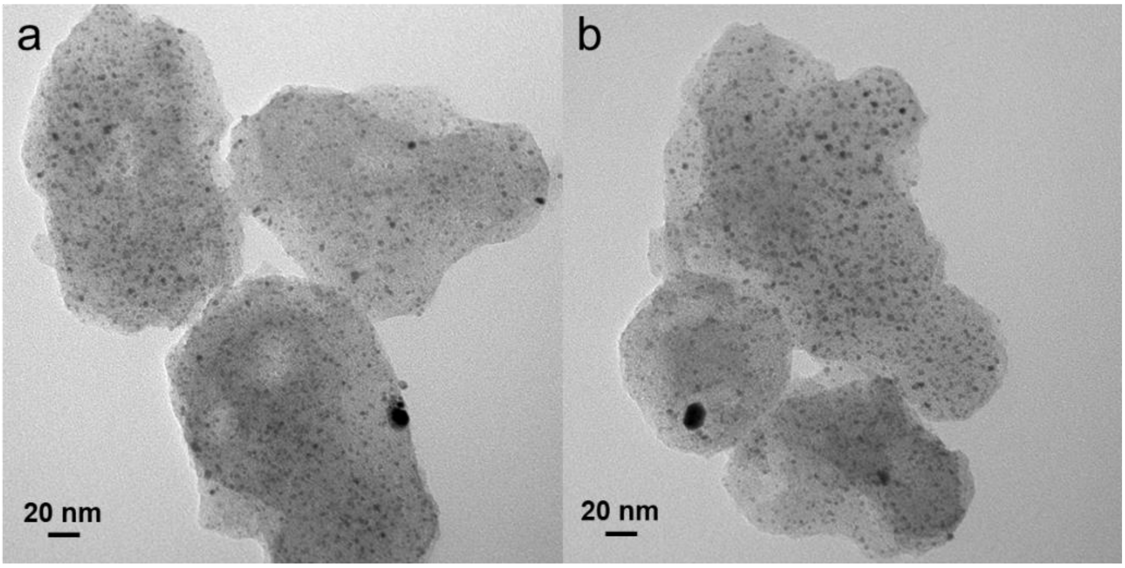

Figure S3 (a-b) TEM images of the nanocomposite.

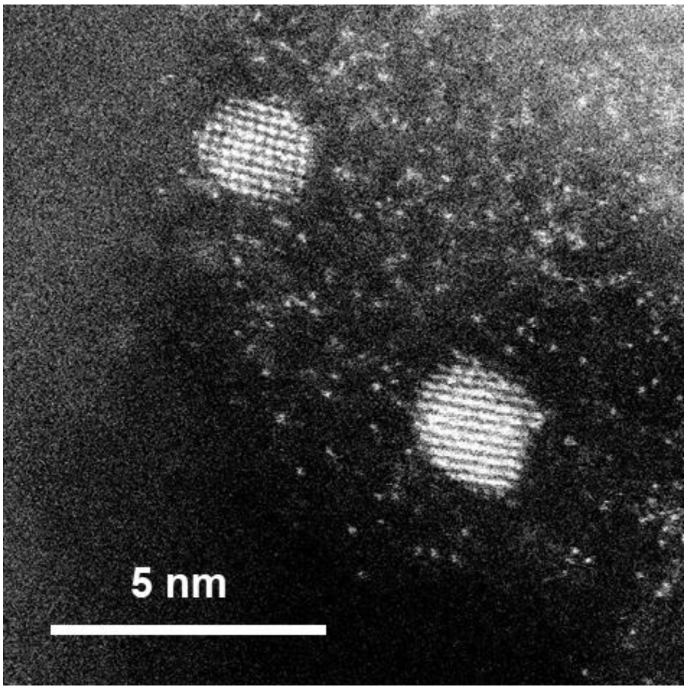

Figure S4 HAADF-STEM image of the nanocomposite.

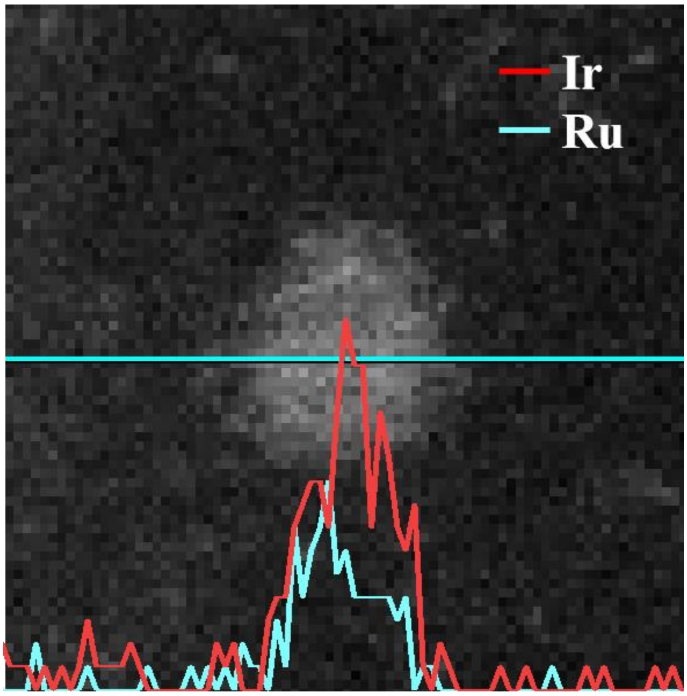

Figure S5 EDS linear scanning profile of an isolated NP in the nanocomposite.

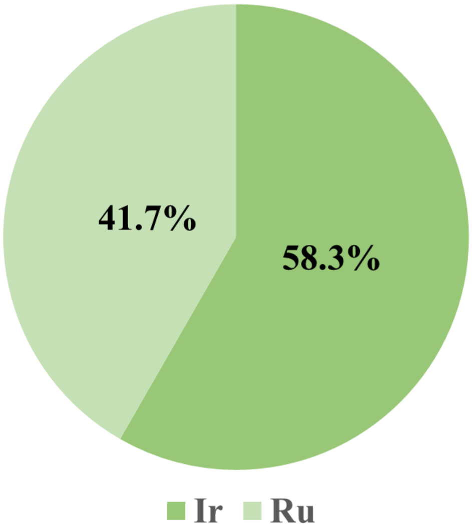

Figure S6 Molar ratio of Ir and Ru of the nanocomposite based on ICP-OES.

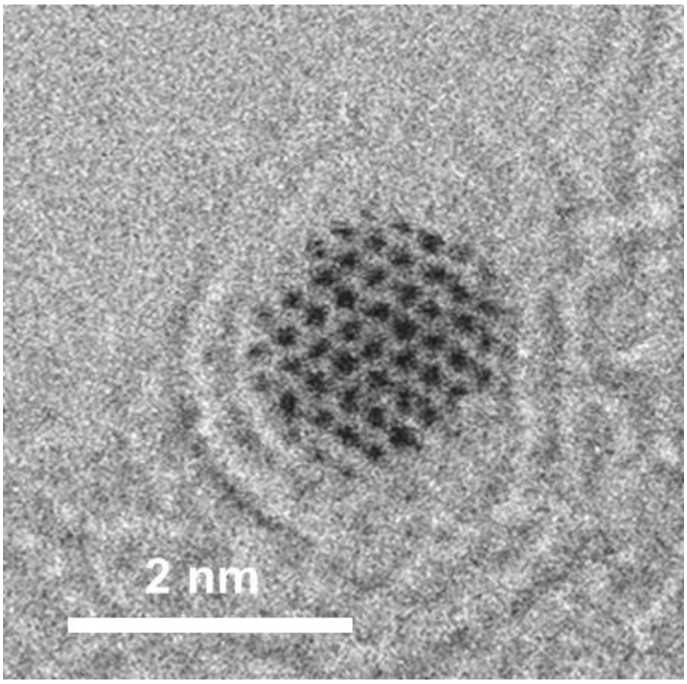

Figure S7 HR-STEM image of a typical IrRu NP.

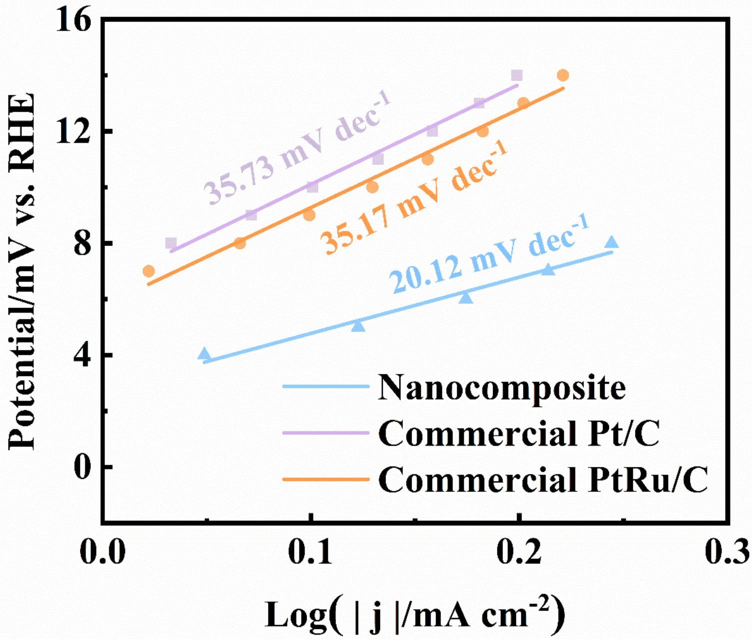

Figure S8 Tafel plots of commercial Pt/C, PtRu/C, and the nanocomposite toward HOR in H_2-saturated 0.5 M H_2SO_4 aq.

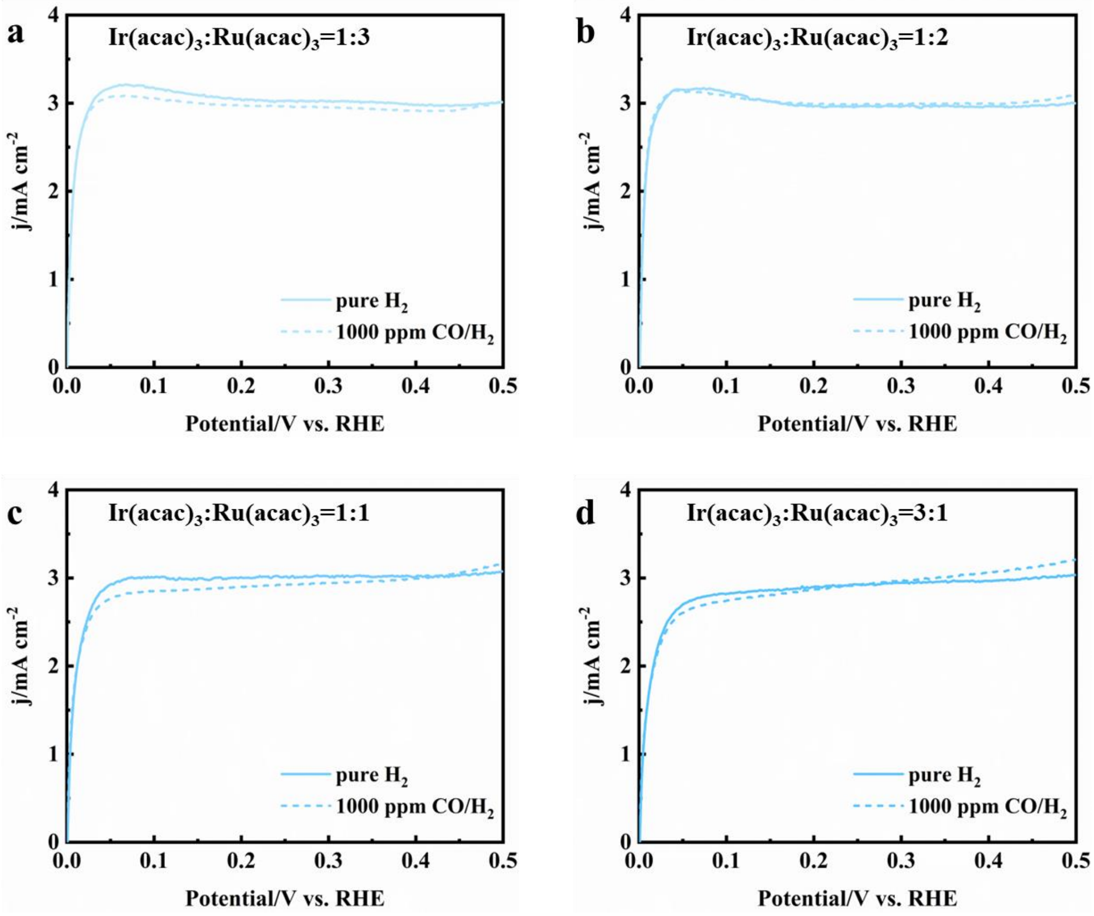

Figure S9 HOR polarization curves of electrocatalysts synthesized with different molar ratios of Ir/Ru precursors (0.5 M H_2SO_4 aq. with/without 1000 ppm CO).

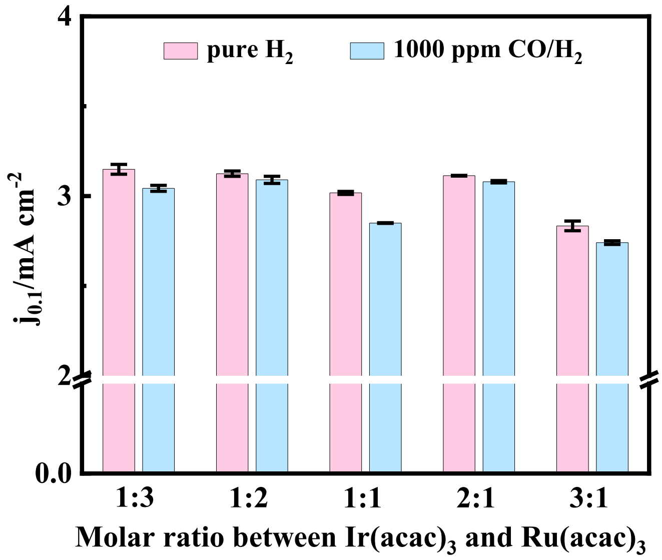

Figure S10 Comparison of $j_{0.1}$ of electrocatalysts synthesized with different molar ratios of Ir/Ru precursors.

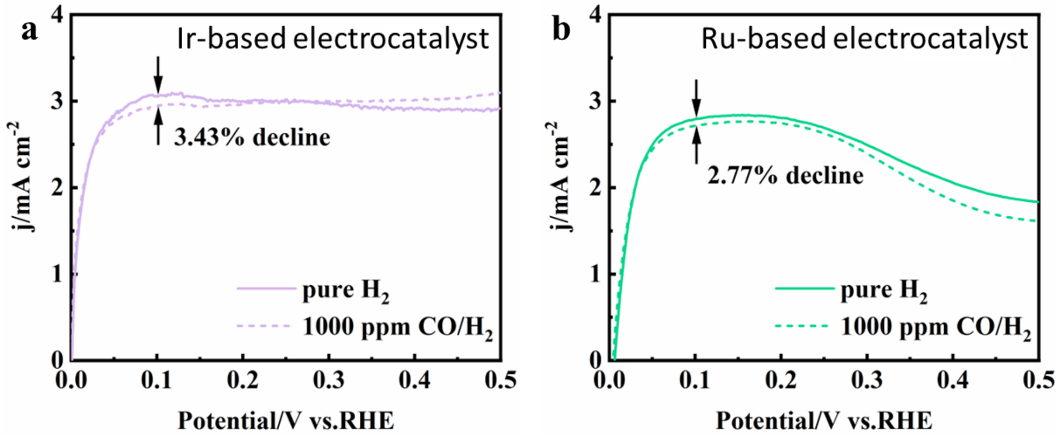

Figure S11 HOR polarization curves of electrocatalysts synthesized with Ir/Ru precursors molar ratios of (a) 1:0 and (b) 0:1, respectively (0.5 M H_2SO_4 aq. with/without 1000 ppm CO).

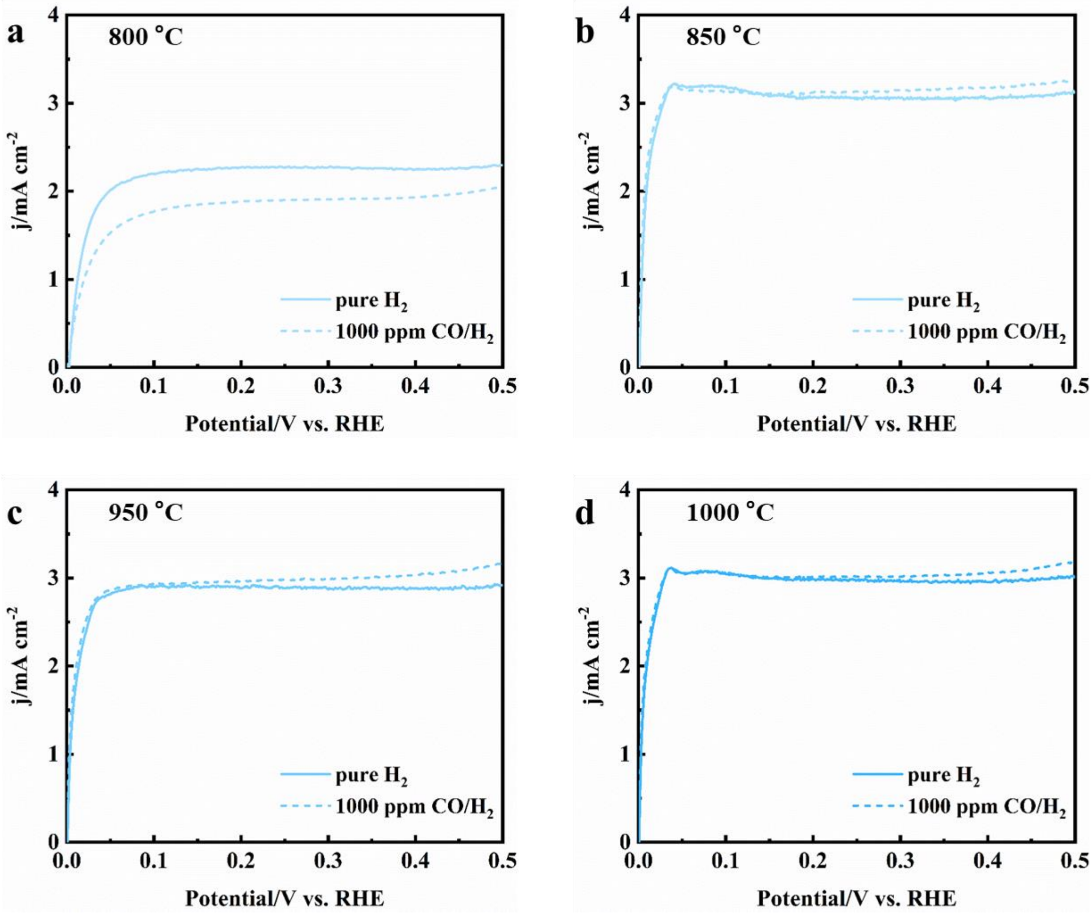

Figure S12 HOR polarization curves of electrocatalysts synthesized with different pyrolysis temperature (0.5 M H_2SO_4 aq. with/without 1000 ppm CO).

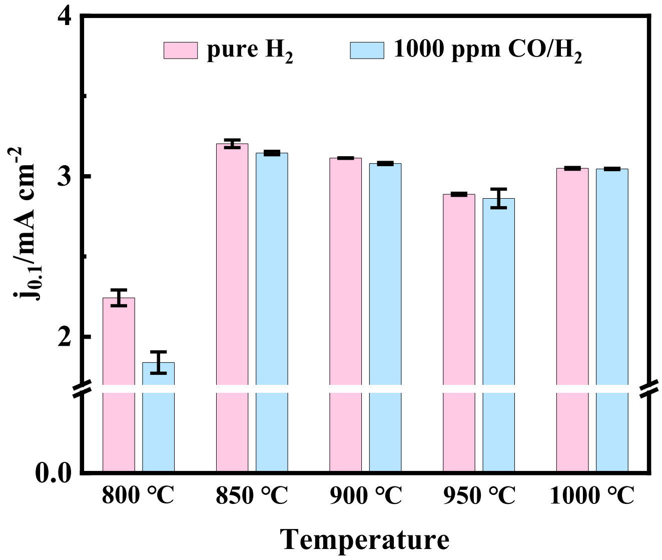

Figure S13 Comparison of $j_{0.1}$ of electrocatalysts synthesized with different pyrolysis temperature.

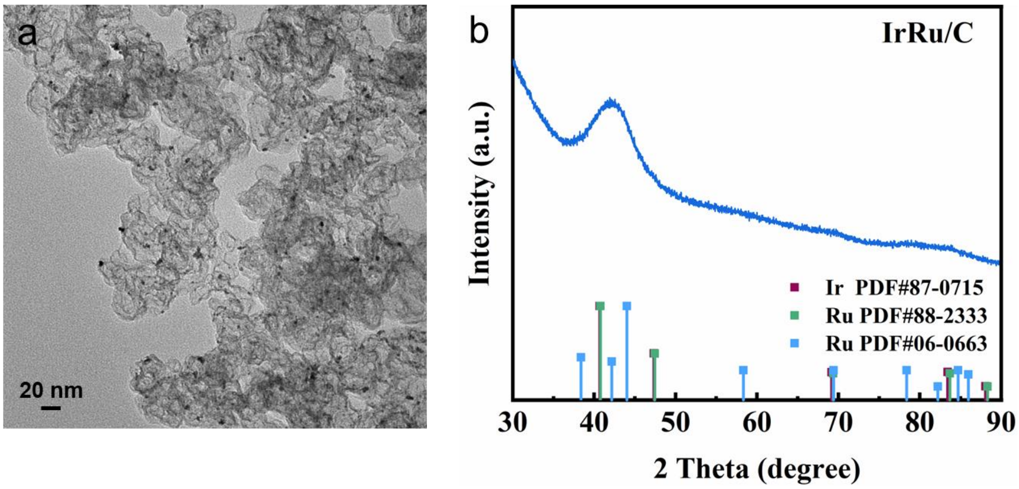

Figure S14 (a) TEM image and (b) XRD pattern of IrRu/C.

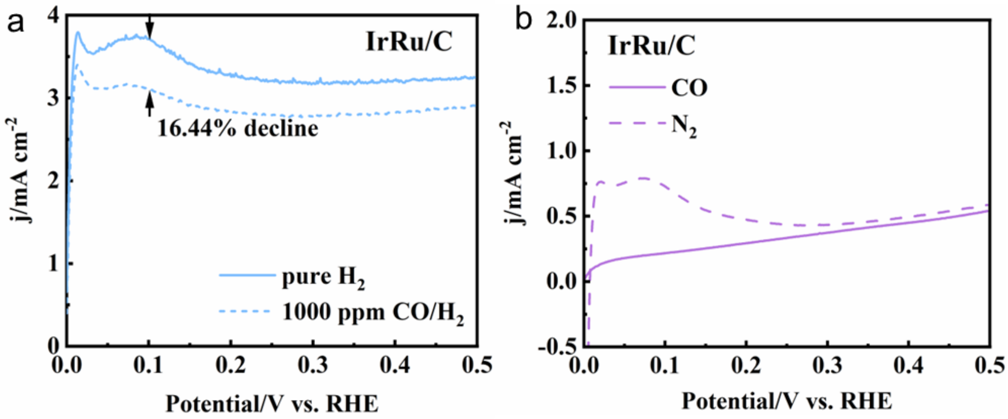

Figure S15 (a) HOR polarization curves of IrRu/C in 0.5 M H_2SO_4 aq. with/without 1000 ppm CO; (b) LSV curves of IrRu/C in CO-saturated 0.5 M H_2SO_4 aq. or N_2-saturated 0.5 M H_2SO_4 aq., respectively.

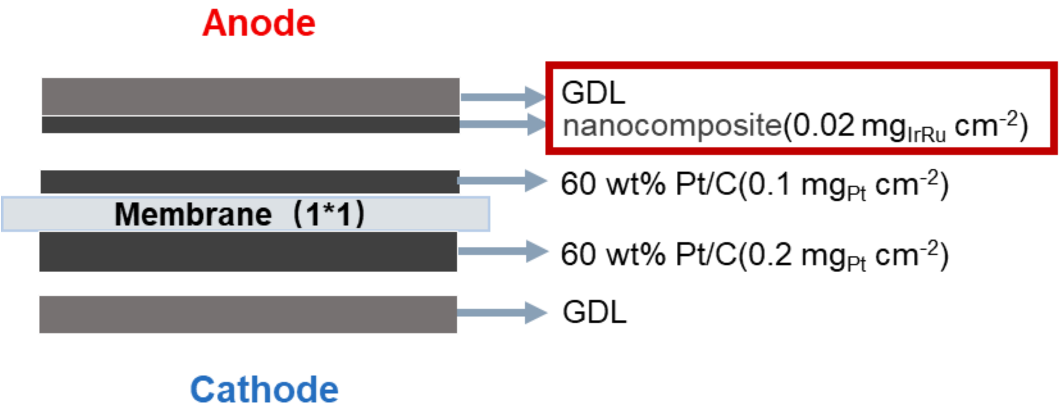

Figure S16 Illustration of the MEA fabricated with the nanocomposite and commercial 60 wt% Pt/C.

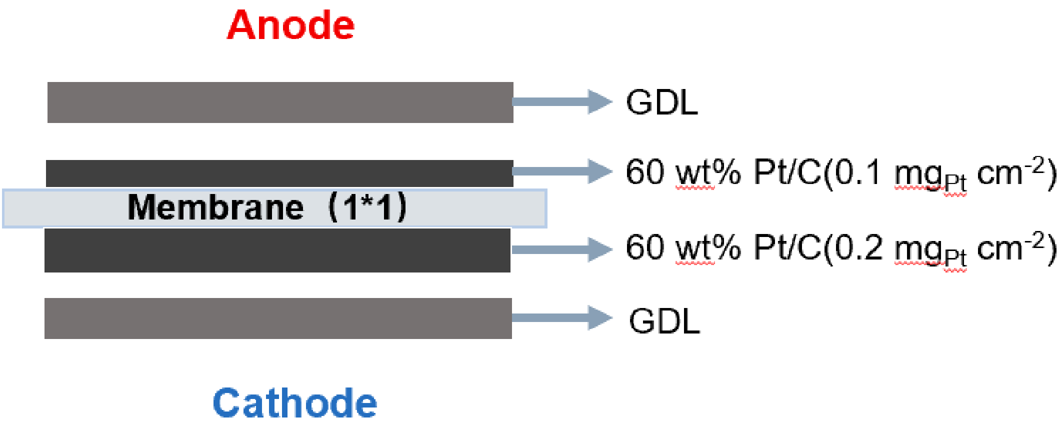

Figure S17 Illustration of the MEA fabricated with commercial 60 wt% Pt/C.

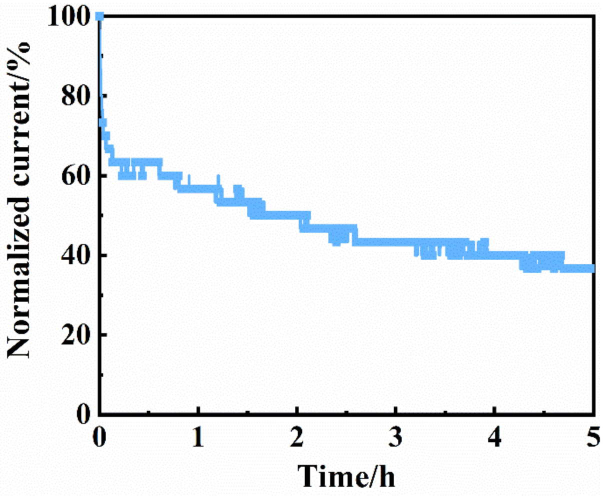

Figure S18 Normalized current of PEMFC at 0.65 V for 5 h.

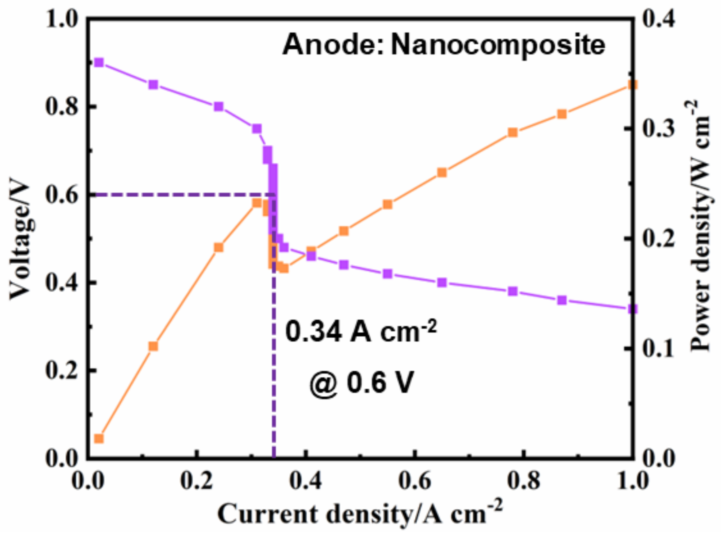

Figure S19 PEMFC performance with the nanocomposite as anodic electrocatalysts. PEMFC operated at 80 °C under 150 kPa with 50 ppm CO/H_2 and O_2.

Table S1. HOR activity of nanocomposite and reported electrocatalysts.

Samples	**The $j_{0.1}$ in H_2-saturated 0.5 M H_2SO_4 aq. (mA cm^{-2})**	**The $j_{0.1}$ in 1000 ppm CO/H_2-saturated 0.5 M H_2SO_4 aq. (mA cm^{-2})**	**Retention rate of $j_{0.1}$ (%)**	**Reference**
Nanocomposite	3.11	3.08	99.04	This work
20 wt% Pt/C	2.54	2.29	90.16	Commercial
30 wt% PtRu/C	2.64	2.37	89.77	Commercial
Pd-WO_3/C	3.70	3.26	88.11	[8]
PtNiMo/Fe-N-C	3.05	2.79	91.48	[9]
Pt-Er/h-NC	2.19	2.07	94.52	[10]
Pt-C-AA	3.13	2.77	88.50	[11]
H-Pt-W_3O/WC	3.18	2.95	92.77	[12]
Pt SACs/CrN	3.01	2.79	92.69	[13]
$PtMo_{10}$/KB	2.90	2.68	92.41	[14]
PtNiW@WO_x	2.92	2.72	93.15	[15]
Pt/W@NCNF	2.80	2.68	95.71	[16]
Ru@TiO_2	2.51	2.46	98.01	[17]
Ir_{NP}@Ir_{SA}-N-C	2.67	2.70	101.12	[18]
IrRh@C_{ZIF-8}	2.60	2.60	100	[19]

Table S2. Stability of nanocomposite and reported electrocatalysts in 1000 ppm CO/H_2-saturated electrolytes.

Samples	**Time of stability test (s)**	**Potential (V vs. RHE)**	**Retention rate of j (%)**	**Reference**
Nanocomposite	2000	0.1	91.68	This work
	3600	0.1	89.69	
20 wt% Pt/C	2000	0.1	23.12	Commercial
30 wt% PtRu/C	2000	0.1	82.02	Commercial
$PtMo_{10}/KB$	1000	0.1	82.98	[14]
$Ir_{NP}@Ir_{SA}$-N-C	1800	0.4	80.6	[18]
$IrRh@C_{ZIF-8}$	2000	0.3	93.6	[19]
Pt/W@NCNF	3000	0.1	74	[16]
H-Pt-W_3O/WC	3500	0.05	98	[12]
Pt SACs/CrN	4000	0.1	91.6	[13]
$PtNiW@WO_x$	4000	0.1	90	[15]

References

1. R. Gao, G. Li, K. Xu, C. Qiu, Y. Cong, Y. Lv, Q. Jiang, J. Qin and Y. Song, *Chem. Commun.*, 2022, **58**, 7309-7312.
2. X. Wang, Y. Li, Y. Wang, H. Zhang, Z. Jin, X. Yang, Z. Shi, L. Liang, Z. Wu, Z. Jiang, W. Zhang, C. Liu, W. Xing and J. Ge, *P. Natl. Acad. Sci.*, 2021, **118**, e2107332118.
3. Y. Lv, H. Liu, J. Li, J. Chen and Y. Song, *J. Electroanal. Chem.*, 2020, **870**, 114172.
4. J. Durst, C. Simon, F. Hasché and H. A. Gasteiger, *J. Electrochem. Soc.*, 2014, **162**, F190-F203.
5. Y. Cong, I. T. McCrum, X. Gao, Y. Lv, S. Miao, Z. Shao, B. Yi, H. Yu, M. J. Janik and Y. Song, *J. Mater. Chem. A*, 2019, **7**, 3161-3169.
6. Y. Liu, L. Cheng, S. Zhou, Y. Yang, C. Niu, T. T. Isimjan, B. Wang and X. Yang, *J. Energy Chem.*, 2024, **94**, 332-339.
7. L. Wei, N. Fang, F. Xue, S. Liu, W.-H. Huang, C.-W. Pao, Z. Hu, Y. Xu, H. Geng and X. Huang, *Chemical Science*, 2024, **15**, 3928-3935.
8. H. Tian, X. Yu, W. Huang, Z. Chang, F. Pei, J. Zhou, N. Dai, G. Meng, C. Chen, X. Cui and J. Shi, *Small*, 2023, **19**, 2303061.
9. Z. Dong, Y. Nan, T. Tang, X.-Z. Liu, J. Fu, H.-R. Pan, Z. Jiang, L. Ding, X. Cheng, L.-R. Zheng, J. Zhang, X. Chang, B. Xu and J.-S. Hu, *ACS Catal.*, 2023, **13**, 7822-7830.
10. G. Chen, W. Chen, R. Lu, C. Ma, Z. Zhang, Z. Huang, J. Weng, Z. Wang, Y. Han and W. Huang, *J. Am. Chem. Soc.*, 2023, **145**, 22069-22078.
11. H. Li, X. Wang, X. Gong, C. Liu, J. Ge, P. Song and W. Xu, *J. Mater. Chem. A*, 2023, **11**, 14826-14832.
12. D. Shen, F. Sun, Z. Liang, B. Mei, Y. Xie, Y. Wang, L. Wang and H. Fu, *Nat. Commun.*, 2025, **16**, 3883.
13. Z. Yang, C. Chen, Y. Zhao, Q. Wang, J. Zhao, G. I. N. Waterhouse, Y. Qin, L. Shang and T. Zhang, *Adv. Mater.*, 2023, **35**, 2208799.
14. C. Jin, Y. Liao, A. Zhang, S. Zhao, R. Wang, J. Li and H. Tang, *Nano Energy*, 2024, **122**, 109305.
15. W. Liu, F. Yang, T. Sun, C. Huang, W. Lai, J. Du, J. Ye, Y. Zeng, L. Gao and H. Huang, *Sci. China Mater.*, 2024, **67**, 1866-1875.
16. X. Zhang, P. Yu, D. Shen, B. Cai, T. Han, Y. Xie and L. Wang, *Adv. Powder Mater.*, 2025, **4**, 100288.
17. Y. Zhou, Z. Xie, J. Jiang, J. Wang, X. Song, Q. He, W. Ding and Z. Wei, *Nature Catalysis*, 2020, **3**, 454-462.
18. X. Yang, Y. Wang, X. Wang, B. Mei, E. Luo, Y. Li, Q. Meng, Z. Jin, Z. Jiang, C. Liu, J. Ge and W. Xing, *Angew. Chem. Int. Ed.*, 2021, **60**, 26177-26183.
19. X. Wang, X. L. Yang, Y. Wang, B. B. Mei, Z. Jin, Y. Li, Z. P. Shi, Z. Jiang, C. P. Liu, W. Xing and J. J. Ge, *Sci. Bull.*, 2024, **69**, 1061-1070.